Cure of Mammary Carcinomas in Her-2 Transgenic Mice through Sequential Stimulation of Innate (Neoadjuvant Interleukin-12) and Adaptive (DNA Vaccine Electroporation) Immunity

Michela Spadaro,[1] Elena Ambrosino,[1] Manuela Iezzi,[2] Emma Di Carlo,[2] Pamela Sacchetti,[1] Claudia Curcio,[1] Augusto Amici,[3] Wei-Zen Wei,[4] Piero Musiani,[2] Pier-Luigi Lollini,[5] Federica Cavallo,[1] and Guido Forni[1]

[1]Department of Clinical and Biological Sciences, University of Turin, Orbassano, Italy; [2]Center of Excellence on Aging Research, "G. D'Annunzio" University Foundation, Chieti, Italy; [3]Department of Molecular, Cellular and Animal Biology, University of Camerino, Camerino, Italy; [4]Karmanos Cancer Institute, Wayne State University, Detroit, Michigan; and [5]Cancer Research Section, Department of Experimental Pathology, University of Bologna, Bologna, Italy

ABSTRACT

Purpose: **Whereas neoadjuvant therapy is emerging as a treatment option in early primary breast cancer, no data are available on the use of antiangiogenic and immunomodulatory agents in a neoadjuvant setting. In a model of Her-2 spontaneous mammary cancer, we investigated the efficacy of neoadjuvant interleukin 12 (IL-12) followed by "immune-surgery" of the residual tumor.**

Experimental Design: **Female BALB/c mice transgenic for the rat *Her-2* oncogene inexorably develop invasive carcinomas in all their mammary glands by the 23rd week of age. Mice with multifocal *in situ* carcinomas received four weekly i.p. injections of 100 ng IL-12 followed by a 3-week rest. This course was given four times. A few mice additionally received DNA plasmids encoding portions of the Her-2 receptor electroporated through transcutaneous electric pulses.**

Results: **The protection elicited by IL-12 in combination with two DNA vaccine electroporations kept 63% of mice tumor-free. Complete protection of all 1-year-old mice was achieved when IL-12-treated mice received four vaccine electroporations. Pathologic findings, *in vitro* tests, and the results from immunization of both IFN-γ and immunoglobulin gene knockout transgenic mice and of adoptive transfer experiments all show that IL-12 augments the B- and T-cell response elicited by vaccination and slightly decreases the number of regulatory T cells. In addition, IL-12 strongly inhibits tumor angiogenesis.**

Conclusions: **In Her-2 transgenic mice, IL-12 impairs tumor progression and triggers innate immunity so markedly that DNA vaccination becomes effective at late points in time when it is ineffective on its own.**

INTRODUCTION

As breast cancer is the most common primary malignant disease in women and often associated with poor prognosis, new strategies for its cure and prevention are urgently needed. There has been a surge of interest in neoadjuvant medical therapy for early breast cancer over the last 10 years in the light of the experience in locally advanced inoperable breast cancer, where systemic treatment before local therapy is now the standard of care (1). Randomized trials comparing neoadjuvant medical and conventional postoperative adjuvant therapy have shown similar rates of local control and overall survival (1–3). These results have been obtained with both chemotherapy and endocrine neoadjuvant therapy, whereas no data are available on the use of antiangiogenic and immunomodulatory agents in a neoadjuvant setting. Microvessel density is an independent and highly significant prognostic factor in breast cancer. Antiangiogenic management designed to prevent the sprouting of new vessels restrains tumor expansion (4). However, although antiangiogenic therapy significantly delays early tumor progression, its contribution to tumor cure is not apparent (5, 6).

Interleukin 12 (IL-12) is a cytokine with a potent antiangiogenic and immunomodulatory activity that elicits numerous downstream proinflammatory cytokines and danger signals, and leads to activation of professional antigen-presenting cells (7). IFN-γ and other downstream cytokines thus elicited inhibit tumor cells, activate potent antiangiogenic mechanisms, and even switch the genetic program of a tumor from proangiogenic to antiangiogenic (7, 8). In many transplantable tumor models, the sum of these activities results in significant inhibition (9, 10). In mice transgenic for the activated rat (r) *Her-2* oncogene (neu and ErbB-2 in humans) under the control of the mouse mammary tumor virus promoter (BALB-neuT), IL-12 delays early carcinogenesis progression, but is not enough to cure established tumors (11, 12). However, it also acts as an essential component of a combined cell vaccine that prevents the early onset of carcinomas (13).

In these mice, adaptive immunity elicited by vaccination with DNA plasmids coding the transmembrane and extracellular domains of r-Her-2 (TMEC plasmids) clears early *in situ* carcinomas and keeps most mice tumor-free (14). This prevention is enhanced when DNA vaccination is boosted by

Received 9/13/04; revised 11/19/04; accepted 12/6/04.
Grant support: Italian Association for Cancer Research, Italian Ministries for the Universities and Health, University of Turin, Compagnia di San Paolo, Turin, and Center of Excellence on Aging, University of Chieti, Italy.
The costs of publication of this article were defrayed in part by the payment of page charges. This article must therefore be hereby marked *advertisement* in accordance with 18 U.S.C. Section 1734 solely to indicate this fact.
Requests for reprints: Federica Cavallo, Department of Clinical and Biological Sciences, University of Turin, Ospedale San Luigi Gonzaga, Regione Gonzole 10, I-10043 Orbassano, Italy. Phone: 39-11-790-5419; Fax: 39-11-236-5417; E-mail: federica.cavallo@unito.it.

r-Her-2^+ IFN-γ-releasing allogeneic cells (15), or when IL-1β fragment (16) or soluble LAG-3 costimulatory molecule (17) are administered concurrently with the vaccine. Moreover, complete prevention is afforded by repeated plasmid electroporations (18).

All these cell and DNA vaccines, however, are ineffective when an invasive carcinoma is established. In the study described in this paper, we determined whether early neoadjuvant stimulation of innate immunity by IL-12 could render effective subsequent DNA vaccination after the onset of carcinomas. The results show that early IL-12 treatment of BALB-neuT mice makes DNA vaccination effective, whereas it is ineffective on its own. This suggests that sequential combination of neoadjuvant stimulation of innate immunity followed by "immune surgery" of the residual tumor cells through induction of adaptive immunity can be proposed as a new and effective strategy.

MATERIALS AND METHODS

Mice. BALB-neuT mice were bred under specific pathogen-free conditions by Charles River (Calco, Italy; ref. 5). BALB-neuT mice knocked out for the IFN-γ (BALB-neuT/IFNγKO), and BALB-neuT mice knocked out for the *immunoglobulin* (Ig) *μ chain gene* (BALB-neuT/μKO) were generated by crossing BALB-neuT mice with BALB/c mice KO for the *IFNγ* gene from The Jackson Laboratory (Bar Harbor, ME), or BALB/c KO mice for the Ig μ chain kindly provided by Dr. T. Blankenstein (Free University, Berlin, Germany; ref. 19). Mice were randomly assigned to control and treatment groups and all groups were treated concurrently. As each experiment was repeated twice to thrice with similar results, data were cumulated and reported. Mammary glands were inspected at weekly intervals to note tumor appearance and tumor masses were measured with calipers in two perpendicular diameters. Progressively growing masses >1 mm mean diameter were regarded as tumors. Tumor multiplicity was calculated as the cumulative number of incident tumors/total number of mice and is reported as mean ± SE (18). Mice were treated according to the European Union guidelines.

Interleukin-12 Administration. Recombinant mouse IL-12 (kindly provided by Dr. Stan Wolf, Genetics Institute, Cambridge, MA) was diluted in PBS supplemented with 0.01% mouse serum albumin (MSA; Sigma, St. Louis, MO) and administered i.p. as previously described (12). Starting from the 7th (7wMSA or 7wIL12) or the 14th (14wIL12) week of age, BALB/c and BALB-neuT mice received a course of one weekly i.p. injection of 0.2 mL PBS containing MSA only (MSA controls) or MSA plus 100 ng of IL-12, for 4 weeks, followed by a 3-week rest. This course was given four times in 7wMSA and 7wIL12 or thrice only in 14wIL12. Other groups of mice were not treated. Because no appreciable differences in tumor growth rate and pathologic findings were found between the untreated mice and the MSA controls, only the data of one of these two groups are shown in Results.

Whole-Mount Image Analyses. Whole mounts of all mammary glands were done as indicated in http://ccm.ucdavis.edu/tgmouse/HistoLab/wholmt1.htm. Digital images were acquired by dividing the whole mount of each gland into 10 quadrants. Ten points were randomly chosen on the duct surface in each quadrant and the corresponding lesions were measured. All lesions with a diameter >150 μm on the same quadrant were counted. Images of whole-mount preparations were taken with a Nikon Coolpix 950 digital camera (Nital Spa, Turin, Italy) mounted on a stereoscopic Leica MZ 6 microscope (Leica Microsystems, Milan, Italy). A 0.63 objective were used to obtain images with a total magnification of ×630 and a resolution of 1,600 × 1,200 pixels. Images were acquired within Adobe Photoshop version 6.0 graphic software (Adobe Systems, San Jose, CA). Glands larger than a single imaging area were captured by photographing contiguous microscopic fields in a raster pattern. Each captured image was merged using the layer technique in Adobe Photoshop to form a single composite image for analysis. Spatial calibration was determined by photographing a 1 mm stage using the same parameters as those for image capturing of whole-mount preparations. The distance drawn on the 1 mm calibration image was divided by 1,000 to find the number of pixels per micrometer. In each image, 100 discrete points were randomly chosen on the duct surface and lesion widths in micrometer were measured perpendicular to duct direction. Points with no lesion were ranked as zero. Lesion measurements were recorded on an Excel spreadsheet and mean and SE were calculated for each treatment group. Statistics were obtained with a two-tailed Student's *t* test.

Preparation of DNA Plasmids. TMEC plasmids were produced as previously described (14–18). For DNA electroporation, 25 μg of TMEC plasmids in 20 μL 0.9% of NaCl with 6 mg/mL polyglutamate were injected bilaterally into the tibial muscle of the hind legs of anesthetized mice. Transcutaneous electric pulses were applied on the shaved skin. Square-wave electric pulses were generated by a T820 electroporator (BTX, San Diego, CA). Two 25 ms pulses with a field strength of 375 V/cm were administered (18).

Evaluation of Serum Vascular Endothelial Growth Factor. Blood samples from groups of three control or treated BALB-neuT mice were collected and the presence of vascular endothelial growth factor in each serum was evaluated with a sandwich ELISA (R&D Systems Inc., Minneapolis, MN).

India Ink Blood Vessel Perfusion and Image Analysis. Groups of three mice were anesthetized and perfused via the left ventricle. An initial blood washout with a solution of 0.5% sodium nitrite and 10 units/mL heparin in PBS at 37°C was immediately followed by reperfusion with black India ink. Fat pads were prepared as whole mounts and stained with carmine. Images of whole-mount preparations were taken as described above with a 4.3 objective giving a total magnification of ×430. At least 10 images were taken for each mammary gland and 25 images from each mouse were randomly chosen for image analysis. The area of the black blood vessel was selected with the Magic Wand Tool in Adobe Photoshop and the number of pixels recorded on an Excel spreadsheet. The width of the blood vessel network is calculated as a percent of total image area.

Histology and Immunohistochemistry. Groups of three mice were sacrificed at the indicated times and samples of mammary tissue or spleen were processed as previously described for immunohistochemical and histologic analysis (20). For immunohistochemistry, acetone-fixed cryostat sections were incubated for 30 minutes with antibodies anti-Mac-1 (CD11b/CD18, clone M1/70.5), anti-CD8 (Ly/T2, clone YT5 169.4) and

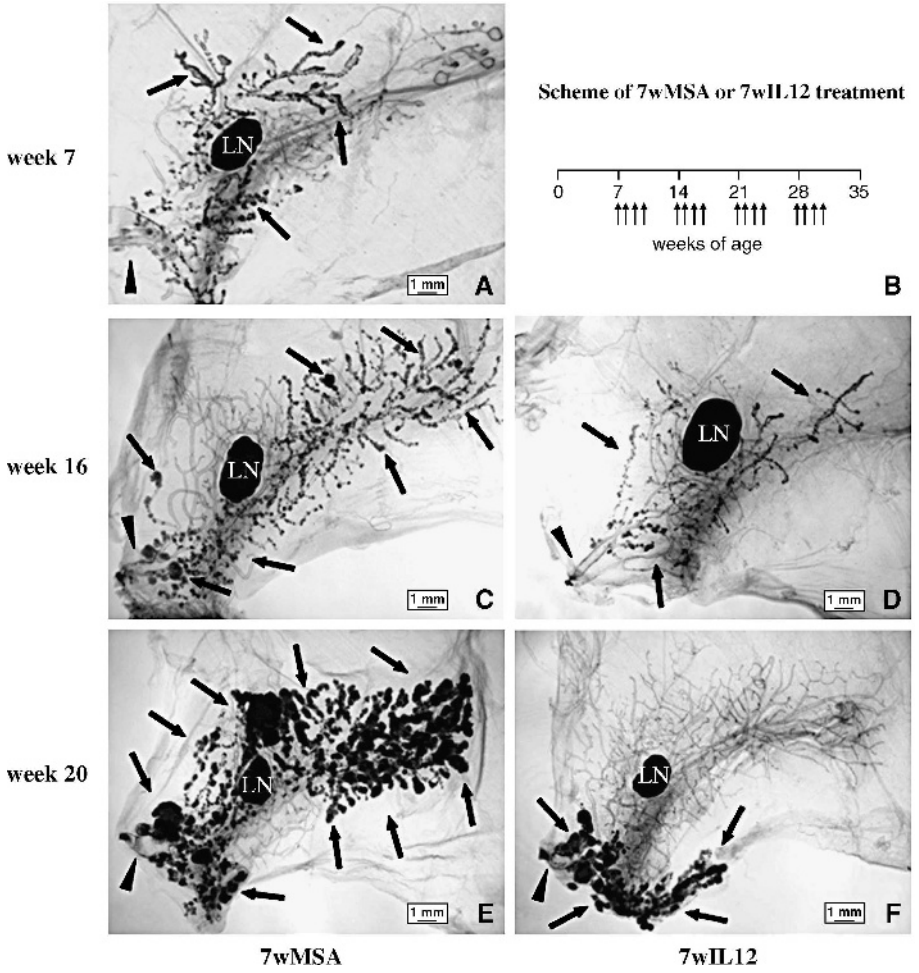

Fig. 1 Whole mounts of the mammary gland documenting the modulation of carcinogenesis in 7wIL12-treated BALB-neuT mice. Numerous neoplastic side bud lesions (*dark spots pointed by the arrows*) are scattered all over the glands of 7-week-old BALB-neuT mice (*A*). Mice with these lesions received an i.p. injection of MSA only or MSA + 100 ng of IL-12 weekly for 4 weeks, followed by 3 weeks of rest. These courses were repeated four times (7wMSA; 7wIL12; *B*). In 7wMSA-treated control mice, the side buds are more diffuse and larger at week 16 (*C*) and coalesce to form multiple masses at week 20 (*E*). In 7wIL12-treated mice, a marked reduction in both the size and diffusion of these side buds is evident at week 16 and week 20 (*D*). At week 20, confinement of the neoplastic lesions close to the nipple is a typical finding. However, the lesions are much larger than at week 16 (*F*). LN, mammary lymph node. (*A-E*, magnification ×63). Three different mice were used for each treatment.

anti-CD4 (LT34, clone YT5.191.1.2; all from Sera-Lab, Crawley Down, Sussex, United Kingdom), or anti-CD11c (clone N418; Chemicon International Inc., Temecula, CA), anti-CD40L (CD154, gp39; clone H-215; Santa Cruz, Biotechnology Inc., Santa Cruz, CA), anti-CD86 (B72, clone PO3), and anti-CD45R/B220 (clone RA3-6B2; all from PharMingen, San Diego, CA), anti-IFN-γ (clone XMG1.2, kindly provided by Dr. S. Landolfo, University of Turin, Turin, Italy). To evaluate the expression of r-p185^{neu} and proliferating cell nuclear antigen, paraffin-embedded sections were tested with polyclonal rabbit anti-Her-2 antiserum (C-18, Santa Cruz Biotechnology) and anti–proliferating cell nuclear antigen (Ylem, Rome, Italy) antibody. After washing, sections were overlaid with biotinylated goat anti-rat, anti-hamster, and anti-rabbit or horse anti-goat Ig (Vector Laboratories, Burlingame, CA) for 30 minutes and incubated with avidin-biotin complex method complex/alkaline phosphatase (DAKO, Glostrup, Denmark). To quantify germinal centers (GC), each spleen was transversely dissected into four segments from which semiserial sections were obtained. The GC in the total area of each section were counted. Morphologic studies were conducted independently by three pathologists in a blind fashion.

Antibody Response. Sera obtained at progressive time points from mice of each treatment group were diluted 1:100 in PBS-azide-bovine serum albumin (Sigma) and the presence of anti-r-p185^{neu} antibody was determined by flow cytometry using BALB/c 3T3 fibroblasts, wild-type, or stably cotransfected with the wild-type r-Her-2, mouse class I *H-2K^{d}* and *B7.1* genes (BALB/c 3T3-NKB). FITC-conjugated goat anti-mouse antibody specific for mouse IgG Fc (DAKO) was used to detect bound primary antibody. Normal mouse serum was the negative control. The monoclonal antibody Ab4 (Oncogene Research Products, Cambridge, MA), which recognizes an extracellular domain of r-p185^{neu}, was used as a positive control. Serial Ab4 dilutions were used to generate a standard curve to determine the concentration (μg/mL) of anti-r-p185^{neu} antibody in serum (12). For isotype determinations, sera from 20-week-old mice were diluted 1:20 and incubated with BALB/c 3T3 and BALB/c 3T3-NKB. Cells were then incubated for 30 minutes with rat biotin-conjugated antibody anti-mouse IgA, IgM, IgG1, IgG2a, IgG2b, IgG3 (Caltag Laboratories, Burlingame, CA). After washing, cells were incubated with 5 μL streptavidin-phycoerythrin (PE; DAKO), and resuspended in PBS-azide-bovine serum albumin containing 1 mg/mL propidium iodide to gate dead cells. Flow cytometry was done with a FACScan (Becton Dickinson, Mountain View, CA). Data were analyzed through CELLQuest (Becton Dickinson) software.

Antibody-Dependent Cellular Cytotoxicity. TUBO cells are a cloned cell line from a carcinoma that arose in a

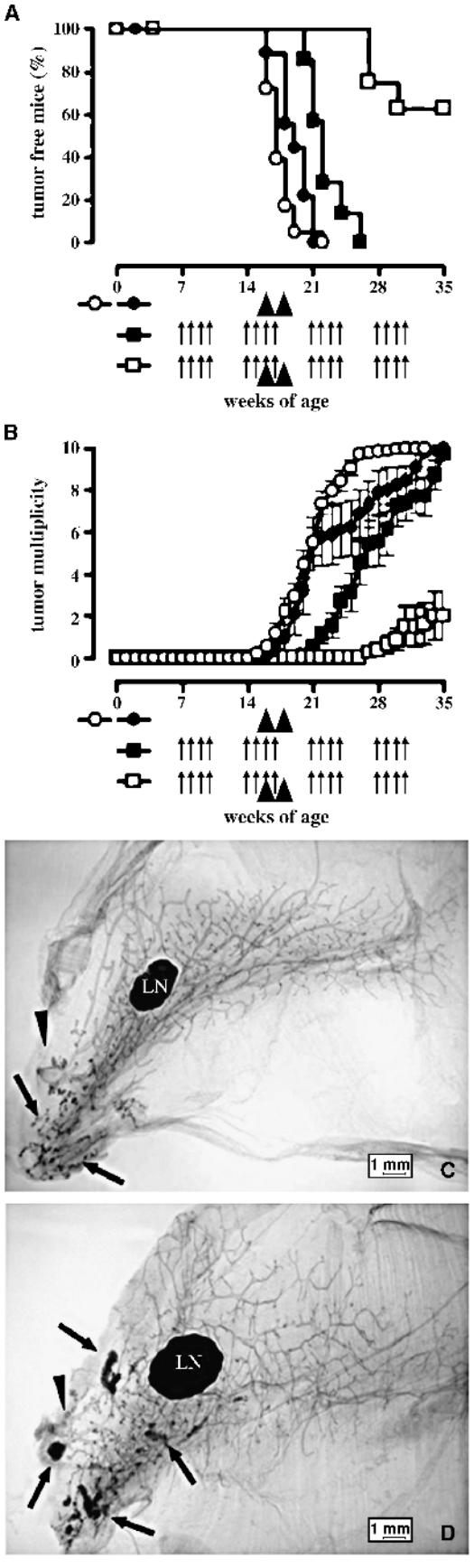

BALB-neuT mouse (14). Five thousand [^{3}H]dTh-labeled TUBO cells were incubated for 2 hours at 4°C with progressive dilutions (1:10 to 1:100) of sera in HBSS (Sigma) and then washed. Effector spleen cells (Spc) from untreated mice were then added at 50:1 effector-to-target ratio to each well of round-bottom microtiter plates (Nunc, Roskilde, Denmark) in triplicate and lysis was determined as previously described (21).

IFN-γ Production. Spc (1×10^7) were stimulated with 5×10^5 mitomycin-C (Sigma) treated TUBO cells in the presence of 10 units/mL recombinant IL-2 (Eurocetus, Milan, Italy). After 4 days, Spc were recovered, washed, and seeded at 2×10^6 cells/mL in the presence of anti-CD28 and anti-CD3 (1 μg/mL final concentration, PharMingen) for 3 hours. IFN-γ-producing cells were identified by using the mouse IFN-γ cell enrichment and detection kit (Miltenyi Biotec, Bergisch-Gladbach, Germany). Recovered Spc were labeled with an anti-IFN-γ (clone R4-6A2) conjugated with an anti-CD45 (clone 30S11) monoclonal antibody (Miltenyi Biotec) for 5 minutes on ice, then incubated for 45 minutes at 37°C. Cross-staining was avoided by keeping the cell density at 1×10^5 cells/mL. IFN-γ bound to the capture matrix was stained with PE-conjugated monoclonal antibody against IFN-γ (clone AN.18.17.24, Miltenyi Biotec). PE-IFN-γ-stained cells enriched with anti-PE microbeads were separated with an autoMACS separator (Miltenyi Biotec). The cells were counterstained with monoclonal antibody against CD4 or CD8α-FITC (clone YTS 191.1.2, clone YTS 169 AG 101 HL respectively; Cedarlane, Hornby, Ontario, Canada) and analyzed by flow cytometry.

Cytotoxicity Assays. Spc (1×10^7) were stimulated for 6 days with 5×10^5 mitomycin-C (Sigma) treated TUBO cells in the presence of 10 units/mL recombinant IL-2 (Eurocetus) and assayed in a 48-hour [^{3}H]dTh release assay at effector-to-target ratio from 50:1 to 6:1 in round-bottomed, 96-well microtiter plates in triplicate (21). The results are expressed as lytic units $(LU)_{20}/10^7$ effector cells, with LU_{20} defined as the number of effector cells needed to kill 20% of the target cells (22).

Adoptive Transfer. Sera and Spc were collected from 20-week-old 7wIL12 + w16-18TMEC BALB-neuT mice. Spc were labeled with a PE-conjugated anti-CD90 monoclonal antibody (clone 53-2.1, PharMingen) and then anti-PE microbeads (Miltenyi Biotec) were used to isolate CD90$^+$ cells with an autoMACS separator (Miltenyi Biotec). Pooled sera (0.5 mL) or

Fig. 2 IL-12 in combination with TMEC plasmid electroporation inhibits the progression of carcinogenesis. Percentage of tumor-free mice (*A*) and tumor multiplicity (*B*) in the w16-18pcDNA3 (○, 18 mice), w16-18TMEC (●, 9 mice), 7wIL12 (■, 7 mice), and 7wIL12 + w16-18TMEC (□, 8 mice) groups. Arrows, week in which IL-12 was injected; arrowheads, week in which plasmids were electroporated. The tumor-free survival curve of 7wIL12 + w16-18TMEC mice is significantly different from that of w16-18pcDNA3 and w16-18TMEC mice (*A*; Mantel-Haenszel test, $P < 0.0001$). The mean tumor multiplicity is significantly lower in 7wIL12 + w16-18TMEC than in w16-18TMEC and w16-18pcDNA3 mice (*B*; Student's *t* test, $P < 0.0006$). At the 20th week of age, the whole mounts of the mammary glands of w16-18pcDNA3 and w16-18TMEC mice show a few small residual side buds (*arrows*), mostly confined to the nipple region (*arrowhead*). At week 34, these lesions are larger (*arrows*), suggesting recommencement of tumor growth (*D*). Oval central black area (*LN*), lymph node (*C* and *D*, magnification ×63). These experiments were done twice.

1×10^7, 90% to 92% $CD90^+$ Spc were administered i.v. in 0.2 mL HBSS to recipient mice at the 10th and 12th week of age. Recipient mice were sacrificed at the 16th week of age and the whole mounts of all 10 mammary glands were evaluated by computer-aided image analysis.

$CD4^+/CD25^+$ T Cells. $CD4^+$ Spc obtained at 20 weeks of age from six mice from each treatment group were purified with the $CD4^+$ T-cell isolation kit (Miltenyi Biotec), separated with an autoMACS separator (Miltenyi Biotec), and then stained with anti-CD4-PE (Cedarlane) and anti-CD25-FITC antibody (clone 7D4, PharMingen). The cells were resuspended in PBS-azide-bovine serum albumin containing 1 mg/mL of propidium iodide to gate dead cells. Flow cytometry was done with a FACScan (Becton Dickinson). Data were analyzed through CELLQuest (Becton Dickinson) software, and reported as the mean of the percentage of $CD4^+/CD25^+$ cells determined in three independent experiments.

Statistics. Differences in tumor incidence were evaluated with the Mantel-Haenszel log-rank test, and those in tumor multiplicity, LU_{20}, IFN-γ-producing Spc, and antibody titer with the two-tailed Student's *t* test.

RESULTS

IL-12 Slows Down Mammary Carcinogenesis. Mammary carcinogenesis follows a very consistent course in virgin female BALB-neuT mice (Fig. 1*A*; ref. 11). When mice with lesions equivalent to atypical hyperplasia and *in situ* carcinoma received recombinant mouse IL-12 i.p. starting from the 7th week of age (7wIL12; Fig. 1*B*), a marked reduction in the progression was already evident at week 16 (Fig. 1*C* versus *D*) and became remarkable at week 20 (Fig. 1*E* versus *F*) when neoplastic side buds were typically confined to the tissue close to the nipple. However, at week 20, the presence of markedly larger lesions (Fig. 1*D* versus *F*) indicates that the protection has vanished and that progression has recommenced. No inhibition was found when IL-12 treatment was postponed to week 14 (14wIL12, not shown).

DNA Vaccination by Electroporation Combined with IL-12 Inhibits Mammary Carcinogenesis. Electroporation *in vivo* of TMEC plasmids when mice display multifocal *in situ* carcinomas inhibits carcinogenesis progression (18), but not if it is postponed to weeks 16 and 18 (w16-18TMEC) when mice already display invasive carcinomas (Fig. 2*A*). By contrast, the combination of 7wIL12 with w16-18TMEC kept 63% of mice free from palpable tumors until 35 weeks when the experiments were ended. Extension of the tumor-free survival was accompanied by a strong reduction in tumor multiplicity (Fig. 2*B*), whereas the whole mounts displayed only a few small residual side buds near the nipple at 20 weeks (Fig. 2*C*). These lesions are markedly smaller than those of mice that received 7wIL12 only (Fig. 2*C* versus Fig. 1*F*). However, at week 35, the presence of larger side buds again points to slow recommencement of progression (Fig. 2*D*). By contrast, all mice remained free of palpable tumors (Fig. 3*A* and *B*) and their whole mounts displayed no signs of tumor progression (not shown) when 7wIL12 + w16-18TMEC mice were further boosted with TMEC plasmids at weeks 23 and 25 (w16-18/23-25TMEC).

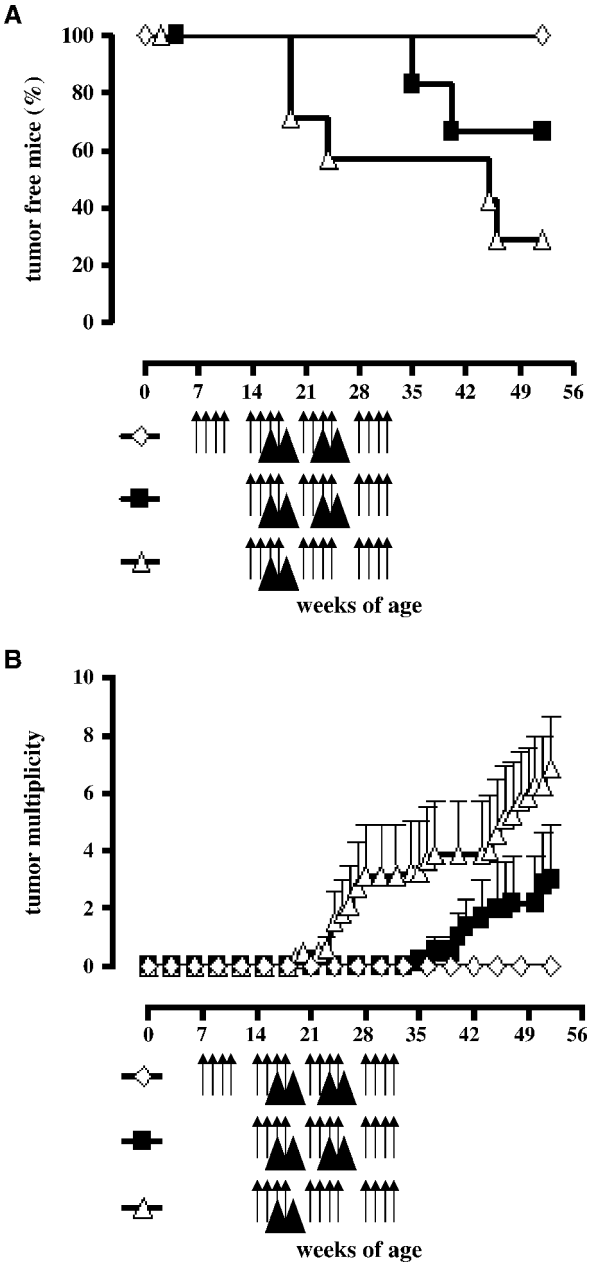

Fig. 3 Successive TMEC plasmid electroporations hamper carcinogenesis even when IL-12 administration is delayed. Percentage of tumor-free mice (*A*) and tumor multiplicity (*B*) in the 7wIL12 + w16-18/23-25TMEC (◇, 10 mice), 14wIL12 + w16-18/23-25TMEC (■, 6 mice), and 14wIL12 + w16-18TMEC (△, 7 mice) groups. Arrow, week in which IL-12 was injected; arrowheads, week in which plasmids were electroporated. The tumor-free survivals in 7wIL12 treated + w16-18/23-25TMEC and 14wIL12 + w16-18/23-25TMEC mice are significantly different (Mantel-Haenszel test, $P < 0.0008$), as are those of 14wIL12 + w16-18TMEC and 14wIL12 + w16-18/23-25TMEC mice (Mantel-Haenszel test, $P < 0.008$). The mean tumor multiplicity is significantly lower in 14wIL12 + w16-18/23-25TMEC mice than in 14wIL12 + w16-18TMEC mice between weeks 36 and 40 (Student's *t* test, $P < 0.05$). Bars, SE of the mean of tumor multiplicity. These experiments were done twice.

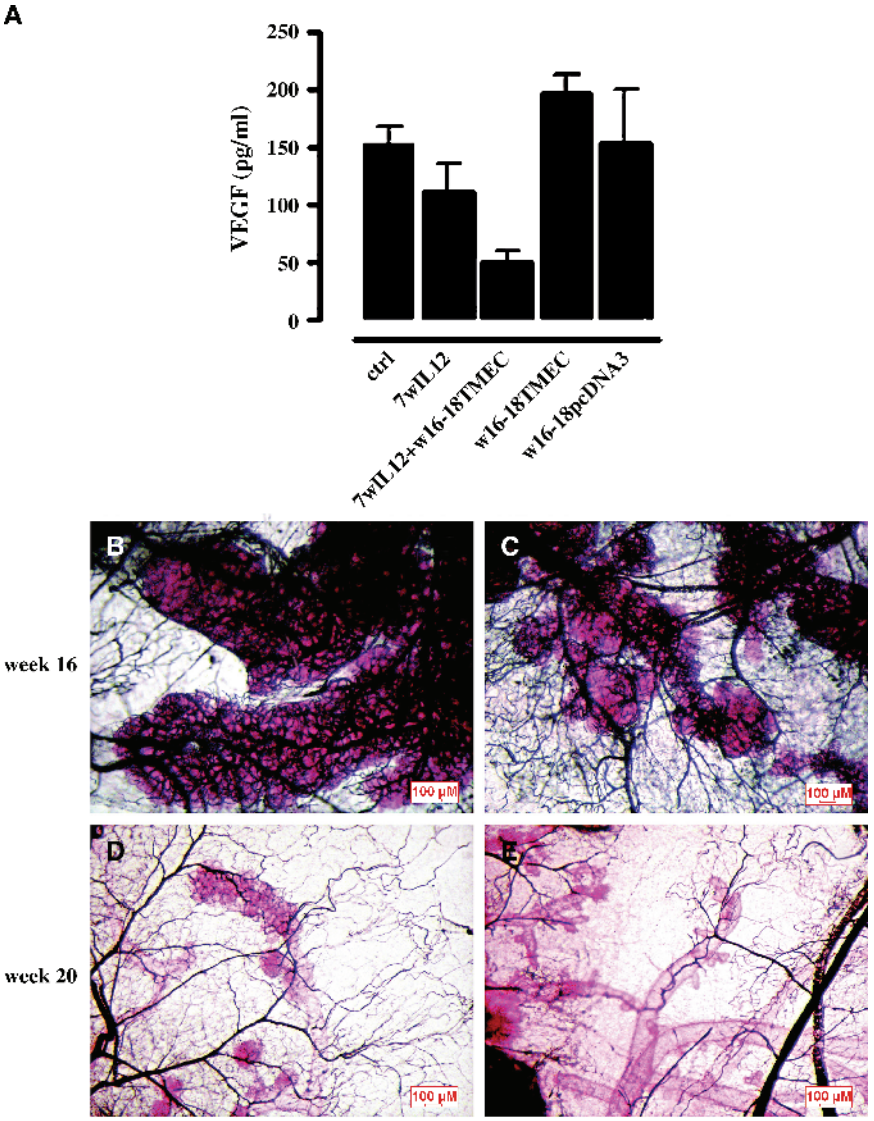

Fig. 4 Antiangiogenic effect of IL-12 treatment + 16-18TMEC in 22-week-old mice. Level of vascular endothelial growth factor in the sera of variously treated mice as assessed by ELISA. Each determination was done on the sera of six mice individually tested (*A*). *B-E,* Perfusion of blood vessels with India ink followed by whole mount of the mammary glands. A widespread vascular network of first-order vessels running longitudinally parallel to the mammary ducts and numerous second-order vessels originating from first-order vessels and penetrating the large neoplastic lesions are evident in control mice (*B*). 7wIL12 alone markedly reduces this network and reduces the size and number of neoplastic lesions (*D*). w16-18TMEC alone slightly decreases lesion size and an increase of small caliber vessels and vascular network is evident around the lesions and in the fat pad stroma (*C*). 7wIL12 + w16-18TMEC leads to a strikingly impressive antiangiogenic effect. Small vessels disappear leaving a network mostly composed of large vessels that accompany breast ducts. Tumor lesions are not evident (*E*). Three different mice were used for each treatment.

In a neoadjuvant setting, IL-12 treatment began when mice already displayed invasive breast cancer (14wIL12) and kept ~70% of mice tumor-free; mice were subsequently vaccinated and boosted (w16-18/23-25TMEC plasmid electroporated mice; Fig. 3). In addition, the combination of neoadjuvant 14wIL12 with week 16 and 18 vaccination (w16-18TMEC) kept 30% of mice tumor-free. No inhibition of tumor takes and multiplicity was found in mice electroporated with pcDNA3 control plasmid at week 16 and 18 only or in combination with 14wIL12 (not shown).

Interleukin-12 Antiangiogenesis. Several immune features were compared among the mice of the various treatment groups to tease apart the immune events that made the DNA electroporation so effective in mice treated with IL-12. These comparisons were made within the 20th and 22nd week of age when whole mounts display the most notable inhibition of tumor progression in treated mice (Fig. 2*C*).

We have previously shown that IL-12 inhibit the angiogenic activity of Her-2^{+} tumor cells *in vitro* (18) and *in vivo* (4). To assess the weight of the antiangiogenic activity of 7wIL12, the amount of vascular endothelial growth factor in the sera of variously treated mice was evaluated (Fig. 4*A*). Whereas a slight decrease in serum vascular endothelial growth factor was found in mice that received 7wIL12 only, the decrease was stronger when 7wIL12 treatment was combined with w16-18TMEC electroporations. This antiangiogenic effect was also notably evident in the whole mounts of mammary glands done after the perfusion of blood vessels with India ink. In 16-week-old mice, 7wIL12 alone leads to a marked decrease of small vessel network (20.85 ± 6.48% versus 36.63 ± 8.88% of total image area ± SD for 7wIL12 and control respectively; $P < 0.003$), associated with a reduction in size and number of neoplastic lesions (Fig. 4*D* versus *B*). Four weeks later, w16-18TMEC electroporation alone lead to a shrinkage of the tumor mass, whereas a vascular network is evident not only around the neoplastic lesions but also in the fat pad stroma (Fig. 4*C*). A strikingly impressive synergistic antiangiogenic (15.29 ± 5.43 versus 41.52 ± 6.14% of total image area ± SD for 7wIL12 treatment + w16-18TMEC and w16-18TMEC alone respectively;

$P < 0.0001$) and an antitumor effect resulted from the combination of 7wIL12 treatment + w16-18TMEC electroporation. Small vessels and neoplastic lesions are no more evident, whereas the vascular mammary network is mostly constituted by large vessels (Fig. 4*E*).

Spleen Germinal Centers and Antibody Response. At 20 weeks of age, the white pulp GC in the semiserial sections of the spleen of 7wIL12 + w16-18TMEC mice were 10 ± 2 per section and 7 ± 2 per section in mice that only received w16-18TMEC. In both cases, GC were significantly more numerous than in mice that received 7wIL12 (3 ± 1 per section) or w16-18pcDNA3 only (2 ± 1 per section; $P < 0{,}001$). In addition, a wider lymphoid white pulp with more expanded B-cell areas and marked B-cell scattering within the T-cell zone are evident in spleens of w16-18TMEC and 7wIL12 + w16-18TMEC mice (Fig. 5*B* and *C*). These morphologic findings on B-cell activation correspond to the serum anti-r-p185^{neu} antibody titers. 7wIL12 + w16-18TMEC mice displayed an earlier, stronger, and much more sustained antibody response to p185^{neu} than w16-18TMEC mice (Fig. 5*D*). Following w16-18TMEC, IgG2a and IgG3 were the most expanded isotypes and IgG1 was the least (Fig. 5*E*). 7wIL12 + w16-18TMEC did not induce an obvious isotype switch, but markedly expanded the production of all isotypes. As these isotypes mediate antibody-dependent cellular cytotoxicity, their ability to guide Spc against r-p185^{neu+} TUBO cells was assessed. Whereas no lysis is observed when TUBO cells are incubated with sera from 7wIL12 or w16-18pcDNA3 mice, those incubated with sera from 7wIL12 w16-18TMEC mice are lysed

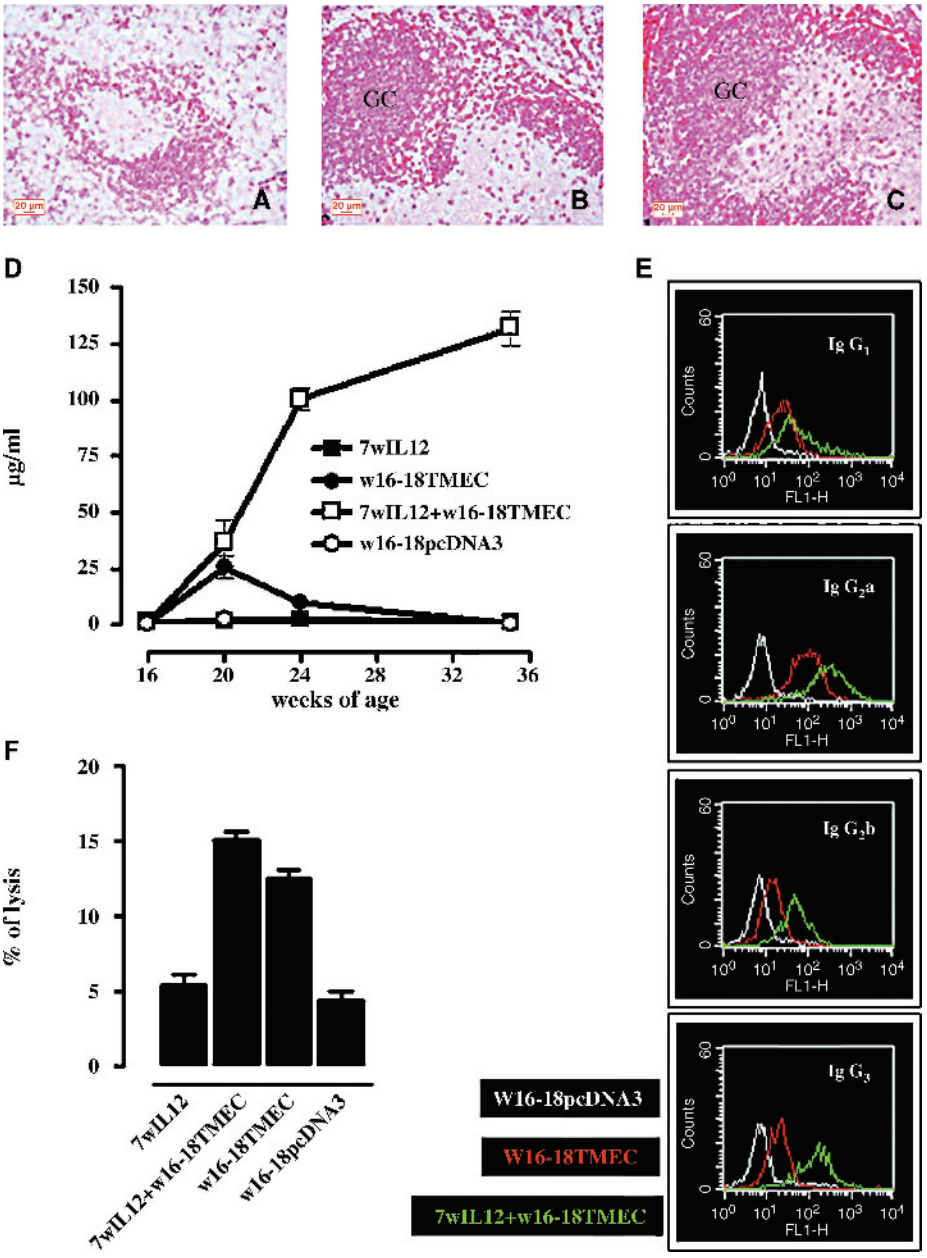

Fig. 5 Effect of 7wIL12 +w16-18TMEC on the anti-r-p185^{neu} B-cell response. Expression of CD45R/B220 B cell marker (*red staining*) in spleens from 20-week-old untreated (*A*), w16-18TMEC (*B*), and 7wIL12 + w16-18TMEC mice (*C*). The lymphoid white pulp is wider with more expanded B-cell areas and frequent GC in the spleen from w16-18TMEC (*B*) and 7wIL12 + w16-18TMEC (*C*) mice. *D,* anti-p185^{neu} antibody in the sera of w16-18TMEC and 7wIL12 + w16-18TMEC mice. The titer is significantly higher in the latter group than in w16-18TMEC electroporated mice, where the titer was significantly higher ($P < 0.0025$ at week 24 and $P < 0.0035$ at week 35). Sera were tested at 1:100; final results in µg/mL have been adjusted for dilution. *E,* isotypes of anti-r-p185^{neu} antibody in the sera (1:20) of w16-18pcDNA3 (*white line*), w16-18TMEC (*green line*), and 7wIL12 + w16-18TMEC (*red line*) mice. *F,* percentage of lysis of r-p185^{neu} target cells in one of three independent antibody-dependent cellular cytotoxicity tests done with pools of sera from five mice bled at week 20. Three different mice were used for each treatment.

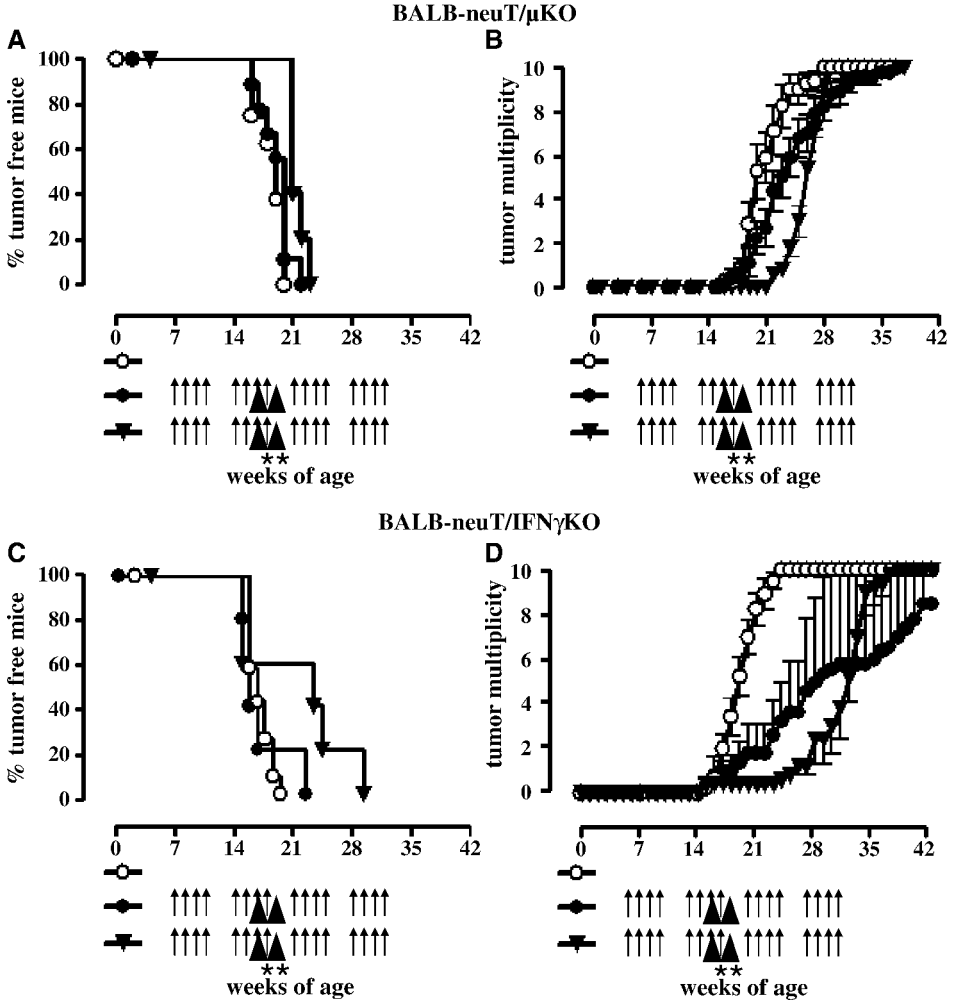

Fig. 6 Effects of 7wIL12 + w16-18TMEC and the transfer of immune sera on the progression of carcinogenesis in BALB-neuT mice deficient for antibody (BALB-neuT/μKO) and IFNγ (BALB-neuT/IFN-γKO) production. BALB-neuT/μKO: percentage of tumor-free mice (*A*) and tumor multiplicity (*B*) of tumors in untreated (○, 8 mice) and 7wIL12 + w16-18TMEC mice (●, 9 mice) and in 7wIL12 + w16-18TMEC mice that received at week 17 and 19 serum from BALB-neuT 7wIL12 + w16-18TMEC mice (▼, 5 mice). Between weeks 22 and 23, 7wIL12 + w16-18TMEC mice displayed a tumor multiplicity that is similar to that of untreated mice but significantly higher ($P < 0.04$) than that of 7wIL12 + w16-18TMEC mice that additionally received immune serum. BALB-neuT/IFN-γKO: percentage of tumor-free mice (*C*) and tumor multiplicity (*D*) in untreated (○, 12 mice), 7wIL12 + w16-18TMEC mice (●, 5 mice), and in 7wIL12 + w16-18TMEC mice that received at week 17 and 19 serum from BALB-neuT 7wIL12 + w16-18TMEC mice (▼, 5 mice). 7wIL12 + w16-18TMEC mice displayed a tumor multiplicity that is significantly lower of that of untreated mice ($P < 0.0001$-0.02) between weeks 19 and 39 but higher of that of 7wIL12 + w16-18TMEC mice that also received immune serum ($P < 0.03$) between weeks 23 and 25. Bars, SE. These experiments were done twice.

in a significantly higher percentage ($P < 0.006$) than those incubated with sera from w16-18TMEC (Fig. 5*F*).

To further assess the significance of antibodies in the inhibition of Her-2 carcinogenesis, BALB-neuT mice with an impaired ability to produce them (BALB-neuT/μKO mice; ref. 18) received 7wIL12 + w16-18TMEC (Fig. 6). The kinetics of mammary carcinogenesis in these mice is similar to that of untreated BALB-neuT mice. Even so, 7wIL12 + w16-18TMEC did not elicit any detectable anti-r-p185^{neu} antibody responses (not shown), nor did it inhibit the onset of carcinoma (Fig. 6*A*), although it led to a marginal and temporary decrease of tumor multiplicity (Fig. 6*B*).

Spleen Dendritic Cells and T-Cell Activation. At 20 weeks of age, immunohistochemical examination of the semi-serial sections of the spleen of untreated mice (Fig. 7*A*) or w16-18pcDNA3 mice (not shown) displays CD11c$^+$ cells with dendritic cell (DC) morphology, mainly at the edge of T-cell areas. These DCs rarely express the B7.2 (CD86) activation marker. 7wIL12 alone gives rise to a marked DC increment and induces preferential CD86$^+$ DC localization at the edge of the T-cell area (Fig. 7*D*), whereas the numerous DCs in the spleen of w16-18TMEC are also scattered along the whole T-cell areas. However, the CD86 activation marker is still preferentially expressed by DC at the edge of the areas (Fig. 7*E*). 7wIL12 + w16-18TMEC mice synergistically increase the number of CD86$^+$ DC at the edge and inside the T-cell areas (Fig. 7*J* and *K*). CD40L is a CD4 T-cell activation marker almost absent in the spleens of untreated (Fig. 7*C*), 7wIL12

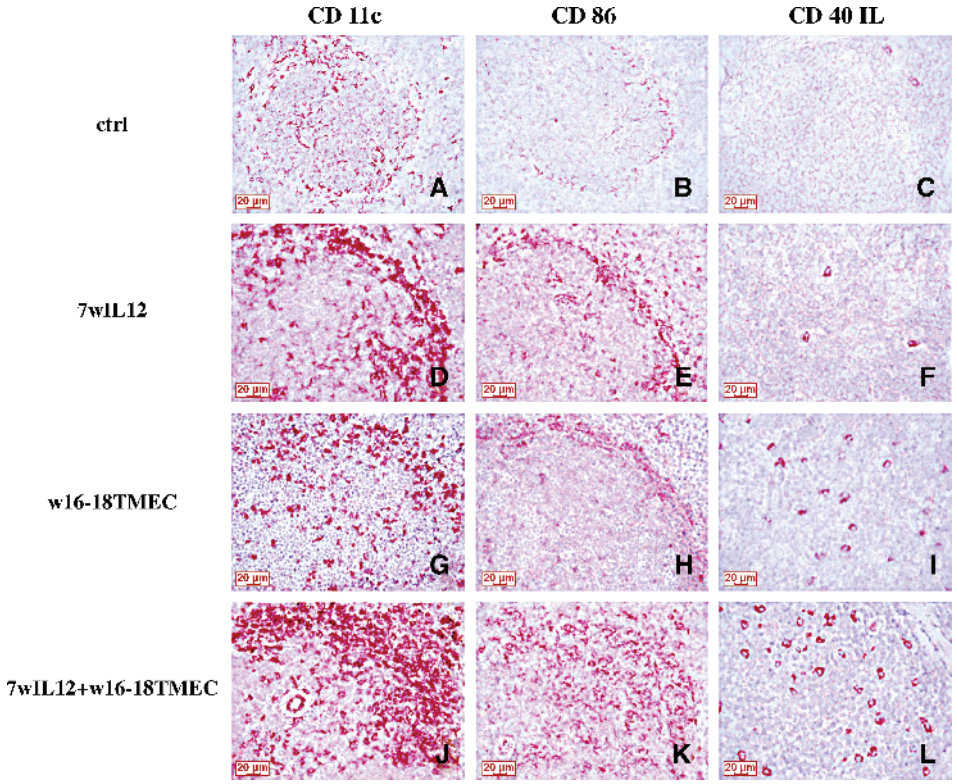

Fig. 7 Effect of 7wIL12 + w16-18TMEC on DC and T-cell activation markers. Expression of CD11c, CD86, and CD40L (*red staining*) in the spleen of 20-week-old untreated and treated BALB-neuT mice. In untreated mice, CD11c-positive cells (DC) are present in the T-cell area and particularly at its edge (*A*) where expression of the activation marker B7.2 (CD86; *B*) is rare. Activated T cells ($CD40L^+$) are almost absent (*C*). 7wIL12 treatment provokes a marked increment of DC, which are preferentially localized at the border of the T-cell area (*D*) and frequently $CD86^+$ (*E*). $CD40L^+$ are scarce (*F*). In w16-18TMEC mice, DCs are more represented than in untreated mice and are found at the edge and scattered throughout the T-cell area (*G*). The activation marker CD86 is preferentially expressed by the borderline DC (*H*). $CD40L^+$ are frequently present and scattered within the T area (*I*). The combined treatment has a synergistic effect on the number and distribution of DC. They are impressively represented (*J*) and diffusely activated (*K*), even in the inner zone of the T-cell area. $CD40L^+$ cells are numerous and scattered within the T area (*L*). Magnification: *A*, *B*, *D*, *E*, *G*, *H*, *J*, *K*, ×400; *C*, *F*, *I*, *L* ×630). Three different mice were used for each treatment.

(Fig. 7*F*), and w16-18pcDNA3 mice (not shown), but frequently expressed in those of w16-18TMEC mice (Fig. 7*I*) and even more in 7wIL12 + w16-18TMEC mice, where it is mostly colocalized with $CD86^+$ DC (Fig. 7*L*).

When the production of IFN-γ by Spc against $p185^{neu+}$ TUBO cells was evaluated with the cytokine secretion assay (Miltenyi Biotec), the frequency of both $CD4^+$ and $CD8^+$ cells producing IFN-γ was much higher in Spc from 7wIL12 + w16-18TMEC (Table 1). This pattern of IFN-γ release correlates with their higher cytotoxic activity compared with all the other treatment groups.

To further assess the weight of IFN-γ, BALB-neuT/IFNγKO mice (13) received 7wIL12 + w16-18TMEC (Fig. 6). The kinetics of mammary carcinogenesis in these mice is similar

Table 1 Effect of 7wIL12 + w16-18TMEC on the IFN-γ production and cytotoxic activity against $p185^{neu+}$ TUBO cells

	w16-18pcDNA3 electroporation	w16-18TMEC electroporation	7wIL12 treatment	7wIL12 treatment + w16-18TMEC electroporation
Percentage of lymphocytes				
Total $CD4^+$*	34 ± 6	21 ± 2	27 ± 1	23 ± 4
Total $CD8^+$	10 ± 3	7 ± 1	8 ± 1	7 ± 1
$CD4^+$ releasing IFN-γ^+	23 ± 7	37 ± 7	16 ± 15	73 ± 15
$CD8^+$ releasing IFN-γ^+	29 ± 7	27 ± 3	30 ± 4	71 ± 16
Cytotoxicity (LU_{20}†) against $p185^{neu+}$ TUBO cells	0.8 ± 0.5	0.5 ± 0.2	10.9 ± 3	41.1 ± 7

*Mean ± SE of the percentage of positive cells as assessed by three independent experiments of flow cytometry.

†Mean ± SE of LU_{20} of Spc from three mice from each treatment group following specific *in vitro* stimulation (7wIL12 versus 7wIL12 + w16-18TMEC, Student's *t* test, $P < 0.05$).

Table 2 Mammary carcinogenesis in recipient BALB-neuT mice to which T cells and serum from 7wIL12 + w16-18TMEC mice were adoptively transferred

	Mean lesion size (μm) ± SD	Number of lesions >300 μm ± SD	Tumor index
Ctrl	246 ± 32	14 ± 12.8	3,444
T cells	169 ± 37	3.1 ± 1.7	524
Serum	102 ± 43	1.16 ± 0.75	118
T cells + serum	127 ± 51	1.33 ± 1.2	169

NOTE. Values of experimental groups are significantly different from control mice ($P \leq 0.0002$) and T-cell treatments are significantly different from serum treatment ($P \leq 0.003$). At least 30 mammary glands of 16-week-old recipient BALB-neuT mice were evaluated in each treatment group. The mean lesion sizes were measured by computer-assisted image analysis in at least 100 randomly selected points without lesions. The tumor index is the product of the mean lesion size and the mean lesion number.

to that of untreated BALB-neuT mice. This combination did not delay the onset of carcinomas (Fig. 6*C*), but tumor multiplicity was transiently reduced (Fig. 6*D*).

Adoptive Transfer. Whole mounts of the mammary glands illustrate the stage of carcinogenesis in BALB-neuT mice. This method was exploited as an intermediate end point to assess the protection provided by the adoptive transfer of antibodies and T lymphocytes. Serum or Spc T cells (90-92% $CD90^+$), isolated by magnetic cell sorting with the autoMACS magnetic separator (Miltenyi Biotec), were collected from groups of 20-week-old untreated control and from 7wIL12 + w16-18TMEC mice. Recipient, otherwise untreated BALB-neuT mice received serum i.p. and T cells i.v. on week 10 and 12 and the whole mounts of their mammary glands were prepared at week 16. The adoptive transfer of T cells and (to a greater extent) serum significantly inhibited carcinogenesis progression (Table 2). The inhibition achieved by the combined transfer of sera and T cells was not significantly different from that obtained with serum alone.

The substantial role of antibodies was also evident in BALB-neuT/μKO and BALB-neuT/IFNγKO mice that received the adoptive transfer of immune serum. In both lines of KO mice, immune serum significantly reduced tumor multiplicity (Fig. 6).

Modulation of T Regulatory Cells. As $CD4^+/CD25^+$ T regulatory cells with suppressive activities are used by the immune system to control its response to self-antigens (23), we investigated their fluctuation during IL-12 treatment and specific immunization. Twenty-week-old w16-18pcDNA3 mice and w16-18TMEC have 14.06 ± 0.49% and 14.16 ± 0.33% $CD4^+/CD25^+$ cells. This number was slightly, but significantly, decreased in 7wIL12 mice (12.65 ± 0.132) and not further decreased (12.597 ± 0.129) by 7wIL12 + w16-18TMEC (Fig. 8).

DISCUSSION

In a preclinical model of multifocal mammary carcinomas, the combination of IL-12 as a neoadjuvant therapeutic agent followed by "immune-surgery" of the residual tumor cells through DNA vaccine electroporation seems able to produce a sustained cure. DNA vaccine electroporation during the early stages of carcinogenesis protects BALB-neuT mice predestined to die of mammary carcinomas (18), whereas later vaccination is totally ineffective. However, combination of early systemic administration of IL-12 with late electroporation provides sustained control of invasive carcinomas, a result that has never been even approached in this devastating model of autochthonous cancer affecting all 10 mammary glands.

The curative potential of this combination seems to be the outcome of the ability of IL-12 to both hamper early carcinogenesis and enhance the specific antitumor immune response (5, 10, 11, 24). The enhancement by IL-12 of the specific protective response elicited by DNA vaccine electroporation fits in well with its powerful adjuvant activity observed with a variety of vaccines against infectious diseases (25). Indeed, induction of IL-12 release is an important mechanism whereby adjuvants exert their effects (26, 27). IL-12 activates innate immune cells and promotes their production of cytokines and chemokines, and thus mediates local recruitment of cells of innate and adaptive immunity (28). Furthermore, an IL-12-conditioned microenvironment is suitable for APC activation, antigen presentation, and prevention (or reversal) of the induction of tolerance toward tumor antigens (29).

In addition, the delay of progression observed when mammary glands display widespread atypical hyperplasia is in line with IL-12-dependent impairment of tumor-driven angiogenesis. The marked inhibition of vascular endothelial growth factor production by 7wIL-12 treatment was somewhat expected, as we have previously observed that IL-12-activated lymphoid cells change gene and protein expression of Her-2 tumor cells and down-modulate their angiogenic activity (8, 10, 11, 30). This inhibition correlates with the dramatic inhibition of the network of small vessels associated with mammary lesions and their hampered progression in 7wIL12 mice. Early IL-12 treatment seems to slow the progression of the incipient tumor and consequently allows the immune response to be more effective against a slow-growing tumor. The significance of tumor angiogenesis as a prognostic indicator has been documented in various kinds of human tumors (31, 32). Tumor vascularity is an indicator of aggressiveness in breast cancer that significantly correlates with its clinical and histologic grades (33).

We have previously shown that an antibody response (5, 8) and production of IFN-γ (13, 15) are essential for successful preventive vaccination. Our present data indicate that combination of IL-12 with DNA electroporation does not obviate the need for an active IFN-γ and antibody response, but markedly enhances the number of T cells that specifically release IFN-γ in the presence of $Her\text{-}2^+$ target cells, the number of spleen GC, the titer of anti-Her-2 antibodies, and the antibody-dependent cellular cytotoxicity. Parallel experiments on wild-type BALB/c mice also showed that 7wIL12 + w16-18TMEC mice produced an anti-Her-2 antibody titer 2-fold of that of mice that received w16-18TMEC only (data not shown). Whereas many of the

downstream factors triggered by systemic IL-12 activate several immune reaction mechanisms and hamper tumor growth (28), IL-12-dependent activation of DC may make a critical contribution to an effective anti-Her-2 response (7). The DC influx and activation at the edge of T-cell areas parallel an increase in activated $CD4^+$ $CD40L^+$ T cells, which release IFN-γ (and probably other cytokines), leading to GC formation and expansions. Moreover, many features of BALB-neuT mice indicate that they are tolerant to the $rp185^{neu}$ (18). Because $CD4^+/CD25^+$ T cells with suppressive activities constitute one of the mechanisms through which the immune system maintains tolerance, we determined whether vaccination schedule reduce their number. Mice treated with IL-12, both alone or in combination with TMEC, display a slight but significant decrease of $CD4^+/CD25^+$ Spc that may contribute to the generation of a good anti-$p185^{neu}$ immune response.

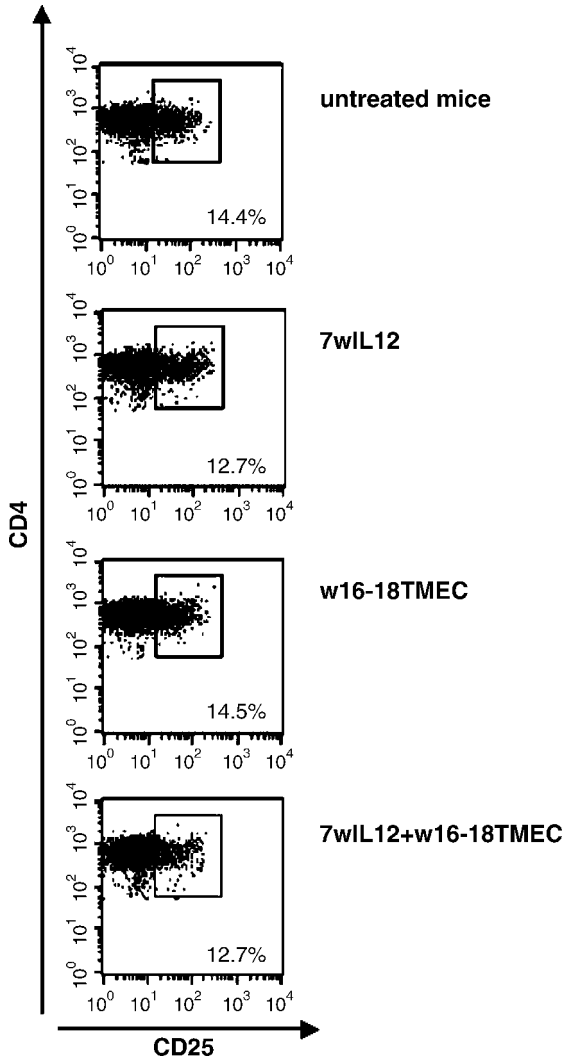

Fig. 8 Reduction of $CD4^+/CD25^+$ T regulatory cells in the spleen of 7wIL12 mice. Spc from 20-week-old untreated, 7wIL12, w16-18TMEC, and 7wIL12 + w16-18TMEC mice were enriched for $CD4^+$ cells and stained with anti-CD25. A representative flow cytometry of three independent analysis of pools of cells from six mice with CellQuest software (Becton Dickinson) is shown. The number of $CD4^+/CD25^+$ cells is consistently reduced in 7wIL12 mice versus w16-18TMEC ($P = 0.011$), and not further decreased in 7wIL12 + w16-18TMEC mice versus w16-18TMEC ($P = 0.011$). Moreover, significant differences were found between 7wIL12 mice versus w16-18pcDNA3 ($P = 0.045$) and 7wIL12 + w16-18TMEC mice versus w16-18pcDNA3 ($P = 0.041$). No differences in the number of $CD4^+/CD25^+$ cells were found between untreated and w16-18pcDNA3 mice (not shown). Three different mice were used for each treatment.

Previous work with transplantable tumors has shown that inhibition of tumor angiogenesis by IL-12 rests on its ability to elicit secondary cytokines and tertiary chemokines and monokines that activate the endothelial cells of neoformed tumor vessels and facilitate leukocyte extravasation (10). These very downstream factors activate innate immunity, enhance the priming of adaptive responses, activate leukocyte subsets that produce proinflammatory cytokines, and induce polymorphonuclear cells to destroy newly formed tumor vessels (28, 30). Combination of distinct antiangiogenic mechanisms intrinsically intermingled with IL-12 immunomodulatory activities leads to the inhibition of both Her-2-dependent tumors in transgenic mice and chemically induced carcinogenesis (24). The resulting delay in tumor progression enables late DNA electroporation to be as effective as early vaccination, as the burden of late mammary lesions is confined to its initial stage. More than 60% of the transgenic mice kept tumor-free by IL-12 in combination with TMEC plasmid electroporation were able to reject a lethal challenge of $p185^{neu+}$ syngenic TUBO cells done 15 weeks after the last DNA vaccination, indicating that this combined immunization also induces a significant and sustained memory response (data not shown).

Early stimulation of innate immunity in humans equivalent to that elicited by IL-12 in mice could delay the progression of a diffuse preneoplastic lesion and allow identification of the target antigens it expresses and the manufacturing of a specific vaccine. Progression will be impeded and the protective potential of the vaccine itself could be significantly enhanced.

ACKNOWLEDGMENTS

We thank Prof. John Iliffe for editing the manuscript.

REFERENCES

1. Shannon C, Smith I. Is there still a role for neoadjuvant therapy in breast cancer? Crit Rev Oncol Hematol 2003;45:77–90.

2. Ring A, Webb A, Ashley S, et al. Is surgery necessary after complete clinical remission following neoadjuvant chemotherapy for early breast cancer? J Clin Oncol 2003;21:4540–5.

3. Smith IE, A'Hein RP, Coombes GA, et al. A novel continuous infusional 5-fluorouracil-based chemotherapy regimen compared with conventional chemotherapy in the neoadjuvant treatment of early breast cancer: 5 year results of the TOPIC trial. Ann Oncol 2004;15:751–8.

4. Kato T, Kameoka S, Kimura T, et al. The combination of angiogenesis and blood vessel invasion as a prognostic indicator in primary breast cancer. Br J Cancer 2003;88:1900–8.

5. Boggio K, Di Carlo E, Rovero S, et al. Ability of systemic IL12 to hamper progressive stages of mammary carcinogenesis in Her2/neu transgenic mice. Cancer Res 2000;60:359–64.

6. Bange J, Zwick E, Ullrich A. Molecular targets for breast cancer therapy and prevention. Nat Med 2001;7:548–52.

7. Trinchieri G. Interleukin-12 and the regulation of innate resistance and adaptative immunity. Nat Rev Immunol 2003;3:133–46.

8. Cavallo F, Quaglino E, Cifaldi L, et al. Interleukin 12-activated lymphocytes influence tumor genetic programs. Cancer Res 2001; 61:2809–12.

9. Brunda MJ, Luistro L, Warrier RR, et al. Antitumor and antimetastatic activity of interleukin 12 against murine tumors. J Exp Med 1993; 178:1223–30.

10. Cavallo F, Signorelli P, Giovarelli M, et al. Antitumor efficacy of adenocarcinoma cells engineered to produce interleukin 12 (IL12) or other cytokines compared with exogeneous IL12. J Natl Cancer Inst 1997;89:1049–58.

11. Boggio K, Nicoletti G, Di Carlo E, et al. Interleukin-12 mediated prevention of spontaneous mammary adenocarcinomas in two lines of Her-2/neu transgenic mice. J Exp Med 1998;188:589–96.

12. Cifaldi L, Quaglino E, Di Carlo E, et al. A light, nontoxic IL12 protocol inhibits Her2/neu mammary carcinogenesis in BALB/c transgenic mice with established hyperplasia. Cancer Res 2001; 61:2809–12.

13. Nanni P, Nicoletti G, De Giovanni C, et al. Combined allogeneic tumor cell vaccination and systemic IL12 prevents mammary carcinogenesis in HER-2/neu transgenic mice. J Exp Med 2001;194:1195–200.

14. Rovero S, Amici A, Di Carlo E, et al. DNA vaccination against rat her-2/Neu p185 more effectively inhibits carcinogenesis than transplantable carcinomas in transgenic BALB/c mice. J Immunol 2000; 165:5133–42.

15. Quaglino E, Rolla S, Iezzi M, et al. Concordant morphologic and gene expression data show that a vaccine freezes HER-2/neu preneoplastic lesions. J. Clin Invest 2004;113:709–17.

16. Rovero S, Boggio K, Di Carlo E, et al. Insertion of the DNA for the 163-171 peptide of IL1β enables a DNA vaccine encoding p185(neu) to inhibit mammary carcinogenesis in Her-2/neu transgenic BALB/c mice. Gene Ther 2001;8:447–52.

17. Cappello P, Triebel F, Iezzi M, et al. LAG-3 enables DNA vaccination to persistently prevent mammary carcinogenesis in HER-2/neu transgenic BALB/c mice. Cancer Res 2003;63:2518–25.

18. Quaglino E, Iezzi M, Mastini C, et al. Electroporated DNA vaccine clears away multifocal mammary carcinomas in Her-2/neu transgenic mice. Cancer Res 2004;64:2858–64.

19. Qin Z, Richter G, Schüler T, et al. B cells inhibit the induction of T cell-dependent tumor immunity. Nat Med 1998;4:627–30.

20. Di Carlo E, Iezzi M, Pannellini T, et al. Neutrophils in anti-cancer immunological strategies: old players in new games. J Hematother Stem Cell Res 2001;10:739–48.

21. Cavallo F, Giovarelli M, Gulino A, et al. Role of neutrophils and $CD4^+$ T lymphocytes in the primary and memory response to nonimmunogenic murine mammary adenocarcinoma made immunogenic by *IL12* gene transfection. J Immunol 1992;149:3677–35.

22. Trinchieri G. Biology of natural killer cells. Adv Immunol 1989; 47:187–376.

23. Shevach EM. $CD4^+$ $CD25^+$ suppressor T cells: more questions than answers. Nat Rev Immunol 2002;2:398–400.

24. Noguchi Y, Richards EC, Chen YT, Old LJ. Influence of interleukin 12 on p53 peptide vaccination against established Meth A sarcoma. Proc Natl Acad Sci U S A 1995;92:2219–23.

25. Gherardi MM, Ramirez JC, Esteban M. Towards a new generation of vaccines: the cytokine IL-12 as an adjuvant to enhance cellular immune responses to pathogens during prime-booster vaccination regimens. Histol Histopathol 2001;16:655–67.

26. Smith RE, Donachie AM, Grdic D, et al. Immune-stimulating complexes induce an IL-12-dependent cascade of innate immune responses. J Immunol 1999;162:5536–46.

27. Portielje JE, Gratama JW, van Ojik HH, et al. IL-12: a promising adjuvant for cancer vaccination. Cancer Immunol Immunother 2003; 52:133–44.

28. Cavallo F, Di Carlo E, Butera M, et al. Immune events associated with the cure of established tumors and spontaneous metastases by local and systemic interleukin 12. Cancer Res 1999;59:414–21.

29. Koido S, Kashiwaba M, Chen D, et al. Induction of antitumor immunity by vaccination of dendritic cells transfected with MUC1 RNA. J Immunol 2000;165:5713–9.

30. Di Carlo E, Rovero S, Boggio K, et al. Inhibition of mammary carcinogenesis by systemic interleukin 12 or p185neu DNA vaccination in Her-2/neu transgenic BALB/c mice. Clin Cancer Res 2001;7:830–7s.

31. Atiqur Rahman M, Toi M. Anti-angiogenic therapy in breast cancer. Biomed Pharmacother 2003;57:463–70.

32. Uzzan B, Nicolas P, Cucherat M, Perret GY. Microvessel density as a prognostic factor in women with breast cancer: a systematic review of the literature and meta-analysis. Cancer Res 2004;64:2941–55.

33. Lipponen P. Ji H, Aaltomaa S, Syrijanen K. Tumour vascularity and basement membrane structure in breast cancer as related to tumour histology and prognosis. J Cancer Res Clin Oncol 1994;120:645–50.